


Research Article

Evolution Mechanism of Water-Conducting Fissures in Overlying Rock Strata with Karst Caves under the Influence of Coal Mining

Wenqiang Wang,^{1,2} Zhenhua Li^{1,2} , Jie Xu,^{1,2} Yue Wang,³ Xuan Fan,^{1,2} and Songtao Li^{1,2}

¹School of Energy Science and Engineering, Henan Polytechnic University, Jiaozuo, 454000 Henan, China

²Collaborative Innovation Center of Coal Work Safety and Clean High Efficiency Utilization, Jiaozuo, 454000 Henan, China

³School of Civil Engineering, Henan Polytechnic University, Jiaozuo, 454000 Henan, China

Correspondence should be addressed to Zhenhua Li; zjlizhenh@163.com

Received 16 March 2022; Revised 12 April 2022; Accepted 27 May 2022; Published 6 June 2022

Academic Editor: Liang Xin

Copyright © 2022 Wenqiang Wang et al. This is an open access article distributed under the Creative Commons Attribution License, which permits unrestricted use, distribution, and reproduction in any medium, provided the original work is properly cited.

There are a large number of karst caves in the limestone rock strata in the karst mining area, and the karst water in rock strata seriously restricts the safe and efficient recovery of coal resources. In order to reveal the influence law of karst caves of rock strata on the evolution of water-conducting fissures in coal seam mining, the numerical simulation method in UDEC software is employed to analyze the development characteristics of water-conducting fissures in coal seam mining under the conditions of karst caves of different sizes. By comparing and analyzing the development characteristics of overlying fissures in rock strata and the displacement fields in coal seam mining under the conditions of different karst caves, the evolution law of water-conducting fissures in coal seam mining is obtained. The research results show that the size of karst cave directly affects the maximum height of the water-conducting fissures in the overlying rock strata in coal seam mining; when the thickness of the coal seam is 3.0 m, the larger the radius of karst cave is, the higher the development height of water-conducting fissures in the overlying rock strata is, and the greater the overall sinking displacement in the Yulongshan limestone is. When the radius of karst cave is between 10 m and 15 m, a through-type water-conducting channel is formed between the working face and the karst cave after the coal seam is mined, and the numerical simulation results are consistent with the field monitoring results. The research results provide an important reference for the prevention and treatment for water inrush disaster in karst mining areas.

1. Introduction

At present, roof water disaster in coal mine is one of the major disasters in China, and roof water disasters cause casualties every year, which poses a serious threat for the safe and efficient production in coal mine [1, 2]. Besides, the karst landform area is developed in coal mining zone, and there are a large number of karst caves in rock strata, especially in Southwest China [3]. Meanwhile, a large amount of atmospheric rainfall enters the karst caves through the karst fissures. When the mining fissures and the water-bearing karst caves are connected, the roof water inrush disaster occurs in working face of coal mine [4, 5]. Therefore, it is of great practical and engineering significance to study the evolution mechanism of water-conducting fissures

in overlying rock strata with karst caves under the influence of coal mining.

In recent years, experts and scholars at home and abroad have done a lot of research on the development law of water-conducting fractured zones in overburden. Wang et al. [6] studied the influence of the structural stability of the main key layer on the evolution of roof water diversion fissures and aquifer water level and obtained the conclusion that the development characteristics of water diversion fissures are different with different fissure forms of the main key layer. Hu et al. [7] studied the relationship between the height of the water-conducting crack and many factors, such as coal seam mining height, hard rock lithology coefficient, working face slope length, mining depth, and mining advance speed. Liu [8] analyzed the relationship between the height of water conducting

crack and the mining thickness of coal seam and drawn the conclusion that there is a positive proportional relationship between the height of the square root of mining thickness. Yang et al. [9] analyzed the height of water-conducting fractured zone of overlying strata under different mining sequences of coal seams. Rong et al. [10] studied the influence of valley slope angle on the movement of roof overburden and the development law of water-conducting fissures in mining the shallow and extrathick coal seam. Wu et al. [11] studied the influence of mining width, mining depth, and advancing speed on the development height of the fractured zone under the condition of fixed mining thickness. Hu et al. [12] studied the relationship between the development height of water-conducting fault zones and coal thickness and working face length during coal seam group mining. Zhu et al. [13] studied the development of mining fissures and the failure characteristics of karst caves in karst mining areas by employing the method of physical similarity simulation. Zhang et al. [14] obtained the failure height of overburden in fully mechanized mining with a large mining height in a deep and thick coal seam in Western Mongolia by employing the methods of field measurement, numerical simulation, and physical similarity simulation. Guo et al. [15] obtained the height of the fractured zone in top coal caving mining under the condition of soft and hard interactive overburden by employing the methods of onsite ground drilling flushing fluid leakage and theoretical analysis. Yang et al. [16] obtained the development height of the fractured zone in fully mechanized top coal caving mining under thick loose layer and soft overburden by comprehensively employing the underground borehole water injection leakage observation, borehole television, and numerical simulation technology. Shi et al. [17] established a PCA-GA-Elman optimization model for predicting the development height of fractured zones, by employing the methods of principal component analysis (PCA), genetic algorithm (GA), and optimized Elman neural network. Li et al. [18] analyzed the ecological, mining, structural, and hydrological conditions in Southwest China and explained the process of rocky desertification driven by coal mining activity in karst mountainous areas. Shi et al. [19] studied the karst development law and groundwater occurrence characteristics of the roof limestone aquifer in Xintian coal mine, by the methods of the controlled-source audiofrequency magnetotelluric method, the water release test, the connectivity test, and water chemical analysis.

At present, most of research results focus on the influence of coal mining on the development height of fissures, and there are some studies on the development law of water-conducting fissures in the karst mining area [20, 21], but there is few research on the influence of the size of karst caves in rock strata on the development height of water-conducting fissures in the karst mining area. Therefore, based on the geological conditions of the Xintian coal mine, this paper adopts the research methods of theoretical calculation and numerical simulation to study the movement of overlying rock strata and the evolution law of water-conducting fissures under the conditions of karst caves of different sizes, which provides a theoretical basis for the safe and efficient production in karst mining areas.

2. Project Overview

2.1. Geological and Mining Conditions. The Xintian coal mine is located in Gantang Township, Qianxi County, Guizhou Province. This area is a typical karst landform area. The karst fissures in ground surface in the mining area are developed. Some surfaces have karst forms such as sinkholes and karst funnels. The comprehensive histogram is shown in Figure 1.

The mining area is characterized by karst development, densely covered sinkholes, karst caves, and rocky desertification. The Yelang formation (T_1y) is divided into the Yulongshan section (T_1y^2) and the Shababaowan section. The Yulongshan section is the whole section of limestone. The upper and middle water diversion channels are developed, and a large amount of precipitation is gathered. It is a strong aquifer, and the lower water diversion fissures are not developed, which creates a weak aquifer; the Shabaowan section is a mudstone layer with good water barrier performance. The limestone of the Changxing Group (P_2c) is located in the lower part of the marl, the shabaowan section, and the development degree of fissures is weaker than that of the Yulongshan limestone, which is a weak aquifer.

The Xintian coal mine is about 8 km long from east to west and 4.6 km wide from north to south. The mining area is 33.4523 km². The mine is developed by the inclined shaft, and the main mining 4# coal seam is now 29.7 m away from the limestone weak aquifer of the Changxing Group and 84.6 m away from the limestone aquifer of the Yulongshan section. The working face adopts the inclined longwall mining method and backward inclined mining, with an annual production scale of 1200000 tons/year.

2.2. Mine Inflow. By comprehensively analyzing the water inflow of the Xintian coal mine from April 2015 to October 2019 and the corresponding atmospheric rainfall in ground surface, it is obtained that the water inflow of the mine is positively correlated with the atmospheric rainfall.

The changing trend of mine water inflow is consistent with the atmospheric rainfall, and the curve change of mine water inflow follows the change of atmospheric rainfall. It is judged that the water inflow of the mine is closely related to the atmospheric rainfall. Atmospheric rainfall is the make-up water source of the mine water, and the mine is connected to the ground. The relationship between mine water inflow and atmospheric rainfall is shown in Figure 2.

There are showers and rainstorms on June 1 and 2, 2019, and the water inflow of the working face is 42 m³/h and 50 m³/h, and the water inflow of the mine surged to 102 m³/h on June 3, 2019. There is less rainfall from June 6 to 15, and the water inflow at the working face shows a steady decline on the whole. However, after the rainfall on June 16, the water inflow at the working face begins to increase. The above analysis further shows that the conduction between the working face and the ground exists. The relationship curve between water inflow and precipitation at the 1402 working face is shown in Figure 3.

The inclined mining method is adopted in the working face of the mine, and the karst water from the roof overburden flows into the working face through the goaf, which not


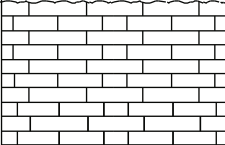
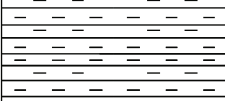
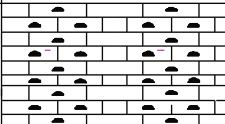


Strata		Columnar	NO.	Thickness (m)	Depth (m)	Rock name	Characteristic
Group	Section						
			1	8.3	8.3	Topsoil	
Yelang group T ₁ Y	Yulong mountain section T ₁ Y ²		2	268.3	276.6	Limestone	Aquifer
	Shabaowan section		3	19.8	296.4	Mudstone	Water barrier
Changxing group P ₂ c			4	35.1	331.5	Limestone	Aquifer
Longtan group P ₂ l			5	29.7	361.2	Sandstone mudstone	
			6	3.0	364.2	4 coal	

FIGURE 1: Comprehensive histogram.

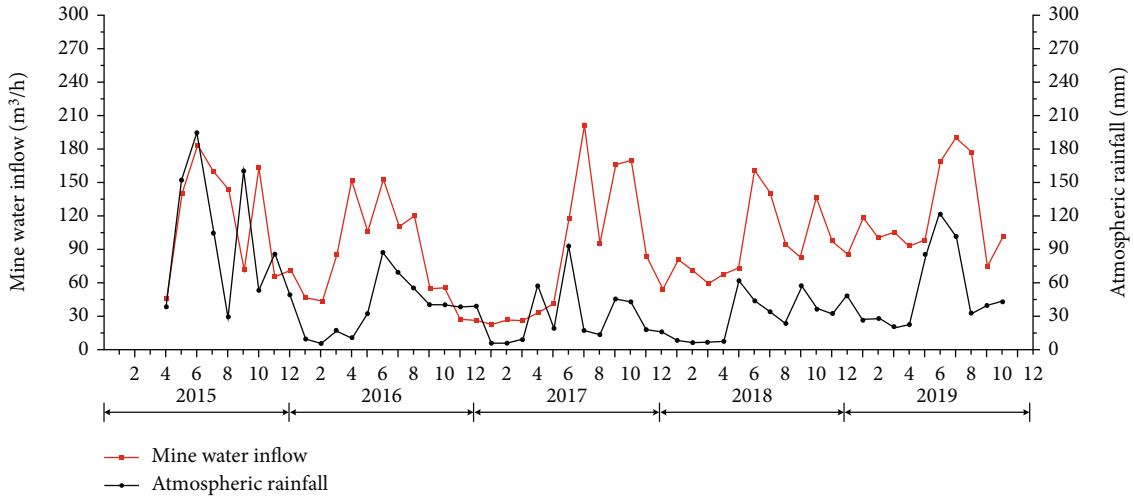


FIGURE 2: Relationship between mine water inflow and atmospheric rainfall.

only reduces the coal quality and causes serious economic losses but also poses a serious threat to safety production in coal mine. Therefore, it is necessary to study the influence of karst caves on the evolution of water-conducting fissures in overburden under the influence of mining.

3. Theoretical Calculation of Development Height of Water-Conducting Fissures

The overlying strata of the 4# coal seam in Xintian Mine include four lithologies, namely, argillaceous siltstone, silty mudstone, limestone, and mudstone, with uniaxial compressive strengths of 50.88 MPa, 53.10 MPa, 59.84 MPa, and 43.08 MPa, respectively. In consideration of the “Specification for Coal Pillar Retention and Coal Briquetting Mining for Buildings, Water Bodies, Railways, and Main Wells and Road-

ways,” most of the rocks are made of hard sandstone, limestone, and sandy rocks in the Mesozoic strata. Shale is mainly made up of conglomerate, tight marl, and iron ore, and the uniaxial compressive strength is in the range of 30-60 MPa. It is judged that the roof of the 4# coal seam is a medium-hard rock layer. When the cumulative mining thickness of the coal seam does not exceed 15 m and the mining thickness of the single layer of coal seam is 1-3 m, the optional calculation equation of the roof water-conducting fractured zone of the medium-hard rock layer is shown in

$$H_{li} = \frac{100\sum M}{1.6\sum M + 3.6} \pm 5.6, \tag{1}$$

$$H_{li} = 20\sqrt{\sum M} + 10, \tag{2}$$

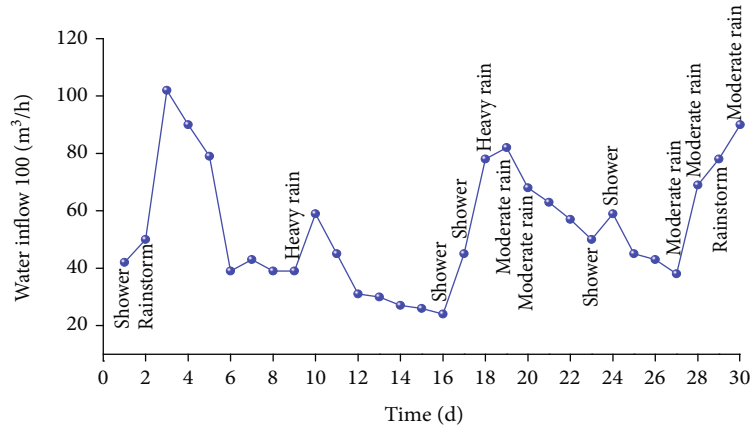


FIGURE 3: The relationship between working-surface water inflow and atmospheric precipitation.

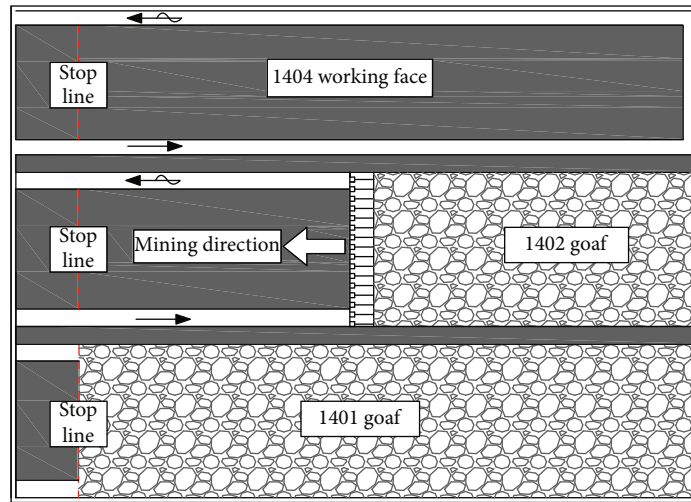


FIGURE 4: Layout of 1402 working face.

where H_{li} is the height of the water-conducting fractured zone and ΣM is the mining thickness of coal seam.

The cumulative mining thickness of the 4# coal seams is 3.0 m, and the empirical equations (1) and (2) are adopted to calculate the height of the water-conducting fractured zone, which is 30.1-41.3 m and 44.6 m, respectively. Therefore, the maximum height of the water-conducting fractured zone is obtained. And it is 44.6 m. According to the comprehensive column chart 1 of the mine, it is obvious that the water-conducting fractured zone develops to the middle of the Changxing Group limestone, which is not connected to the Yulongshan limestone aquifer and is positively correlated with the mine water inflow and atmospheric rainfall. The distance from the 4 # coal seam to the Yulongshan limestone aquifer is 84.6 m, which is much larger than the calculated height of the maximum water-conducting fractured zone of 44.6 m. It is connected to the limestone aquifer of Changxing Group on the roof and the limestone aquifer of Yulongshan Member. Therefore, the calculation equation is no longer suitable under the karst roof conditions in Xintian coal mine.

4. Numerical Calculative Models

4.1. Overview of Test Working Face. The 1402 working face in Xintian coal mine is selected as the test working face. The mining 4# coal seam of this working face has a strike length of 147 m, a mining dip length of 930 m, a buried depth of 340-376 m, an average mining thickness of 3 m, and an average dip angle of 3° . The east side of the working face is 1401 goaf, and the west side is 1404 unprocessed working face. The layout of 1402 working face is shown in Figure 4.

4.2. The Establishment of Numerical Model. According to the geological exploration data of the mine, a large number of beaded karst caves and karst fissures are stored in the limestone aquifer of Yulong Mountain, but the specific conditions of karst storage are difficult to explore. To explore the influence of karst caves on the evolution process of overburden water-conductive fissures, the karst caves are simplified to circular, and the numerical models of karst caves with different radius are established through the discrete element

TABLE 1: Numerical simulation of physical and mechanical parameters.

Rock formation	Thickness (m)	Bulk modulus (GPa)	Shear modulus (GPa)	Density ($\text{N}\cdot\text{m}^{-3}$)	Angle of internal friction ($^{\circ}$)	Group cohesiveness (MPa)	Tensile strength (MPa)
Yulong mountain limestone	268	31.93	18.25	2960	57.51	6	8.59
Mudstone	20	8.23	4.70	2630	31.73	1.1	1.53
Changxing group limestone	35	31.93	18.25	2960	57.51	6	8.59
Silty mudstone	27	25.81	14.02	2690	50.77	4.07	6.82
Argillary siltstone	3	23.64	12.85	2820	44.82	3.08	7.41
4# seam	3	1.19	0.82	1450	25	1.3	1.79

TABLE 2: Numerical simulation test scheme.

Scheme	Mining thickness (m)	Cross-sectional shape	Round caves radius (m)	Proportion of the limestone layer of Yulong Mountain
1	3	—	—	0
2	3	Rotundity	5	0.88%
3	3	Rotundity	10	3.51%
4	3	Rotundity	15	7.91%

numerical simulation software UDEC6.0 to simulate the influence of karst caves of different scales on coal seam mining and the development of water-conducting fissures. The numerical simulation of the physical mechanics parameters is shown in Table 1.

According to the mining geological conditions in 1402 working face of Xintian coal mine, the top plate of the 4# coal seam has a rock layer of 353 m and a topsoil layer of 8 m, and the bottom plate has a sandstone layer of 36 m, and the total thickness of the model is 400 m. Therefore, the two-dimensional numerical model size is $400\text{ m} \times 400\text{ m}$, and a total of 4 sets of numerical models are established, namely, the complete model; the karst cave model with a radius of 5 m, a radius of 10 m, and a radius of 15 m; and the proportion of the cave in the total space of the limestone layer in Yulongshan, shown in Table 2.

To ensure the uniqueness of the study variables, each model contains 12 karst caves, and the center of each karst cave is a fixed point. The horizontal distance between the center points of circular caves is 100 m, and the vertical distance is 67 m. The schematic diagram of the numerical model test scheme is shown in Figure 5.

5. The Influence of Karst Caves on Evolution of Water-Conducting Fissures

5.1. Analysis of Evolution Characteristics of Water-Conducting Fissures

- (1) Water-conducting fissure development characteristics in nonkarst caves

When the working face is advanced by 45 m, the development height of the mining fissure is 21 m; when the working face advances by 60 m, the development height of the

water-conducting fissured zone is 44 m. Mining-induced fissures developed in the middle part of the limestone, and the middle part of the Changxing Group limestone and sand-mudstone produce large abscission fissures; when the working face is advanced by 120 m, the water-conducting fissures develop to a height of 85 m, and the mining fissures develop to the bottom of Yulongshan limestone; when the working face is advanced by 280 m, the height of the water-conducting fissure is 95 m, and the working face reaches full mining state. At this time, the mining fissure develops to its maximum height, which is 10 m away from the bottom boundary of Yulongshan limestone. The development characteristics of water-conducting fissures under the condition of no karst caves are shown in Figure 6.

- (2) Development characteristics of aqueducts in karst caves

- (1) The radius of the karst cave is 5 m

When the working face is advanced by 45 m, the development height of the water-conducting fractured zone is 21 m; when the working face is advanced by 120 m, the height of the water-conducting fractured zone is 85 m; the water-conducting fissure layer appears at the bottom boundary of the Yulongshan limestone layer; when the working face is advanced by 280 m, the working face reaches full mining state. At this time, the development height of the mining fissures is 115 m, and the fissures develop to the bottom of the Yulongshan limestone. The karst cave does not collapse, and there are only small mining disturbance fissures around. When the radius of the karst cave is 5 m, the mining of the 4# coal seam does not cause damage to the overall structure of the limestone. The development characteristics of water-conducting fissures when the karst cave is 5 m are shown in Figure 7.

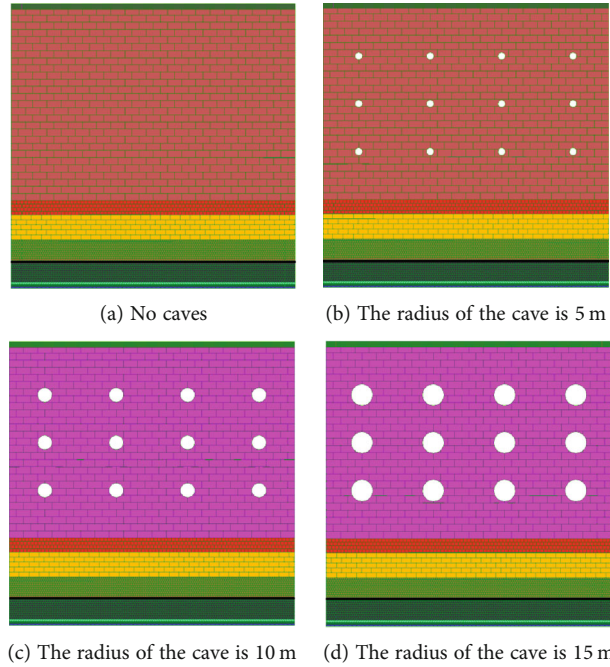


FIGURE 5: Schematic diagram of the numerical model test scheme.

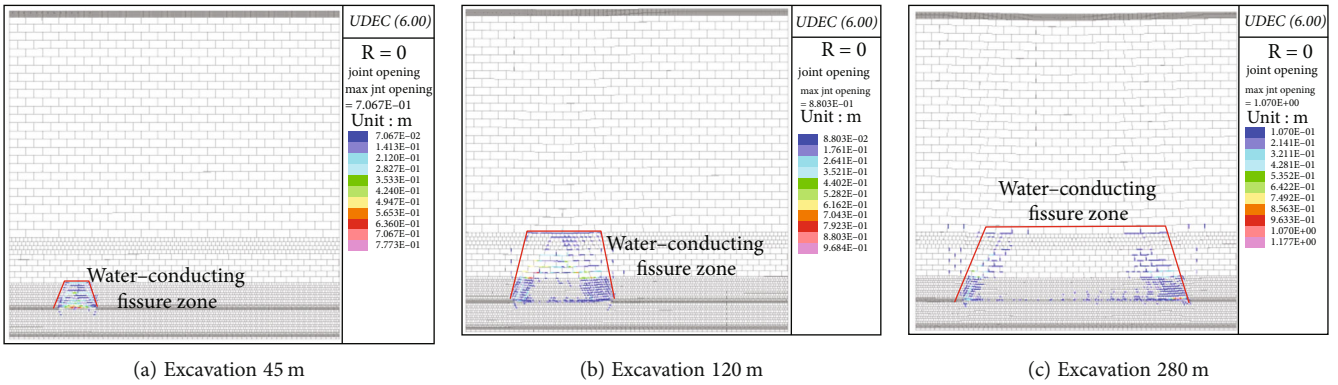


FIGURE 6: Development characteristics of water-conducting fissures under the condition of no karst caves.

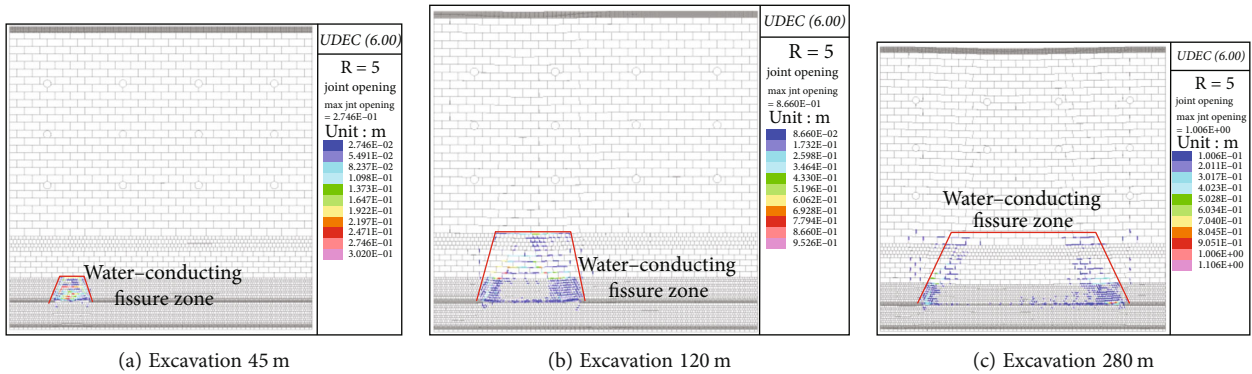


FIGURE 7: Development characteristics of water-conducting fissures when the karst cave is 5 m.

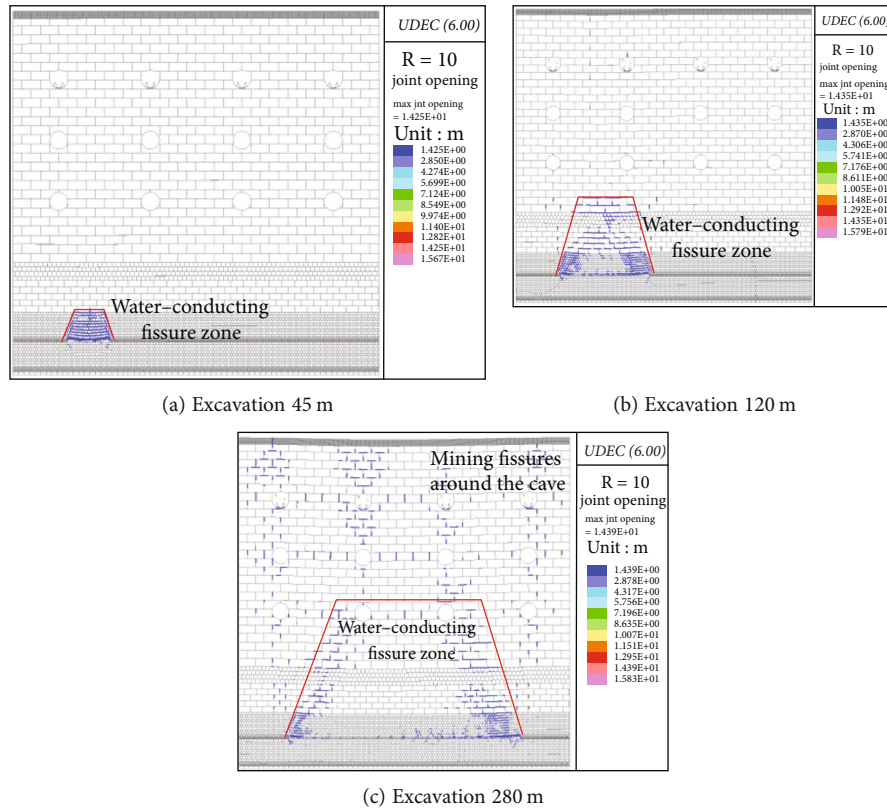


FIGURE 8: Development characteristics of water-conducting fissures when the karst cave is 10 m.

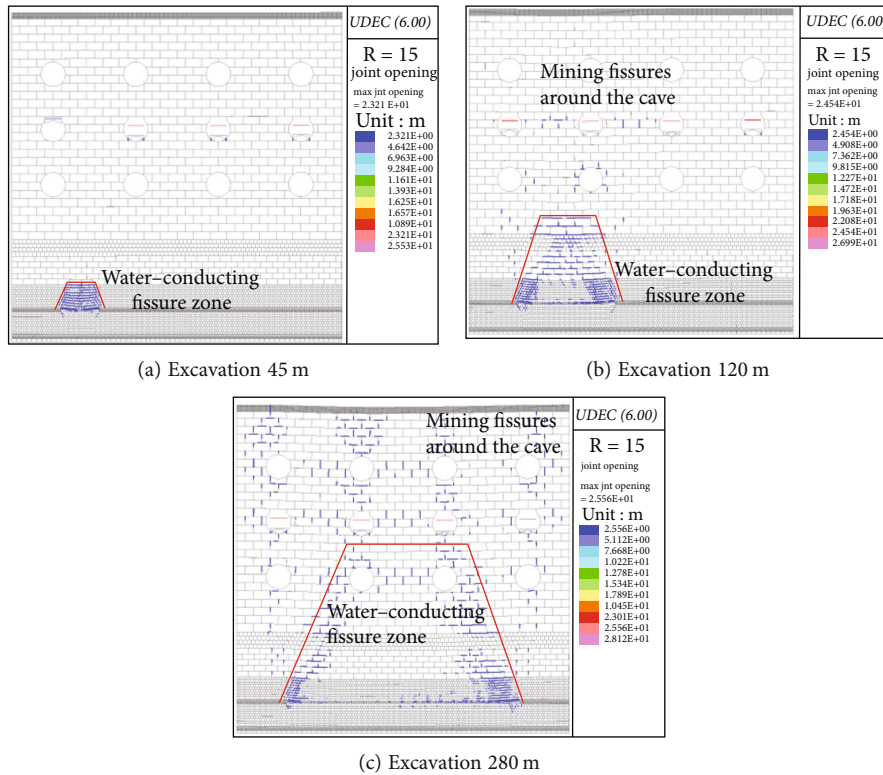


FIGURE 9: Development characteristics of water-conducting fissures when the karst cave is 15 m.

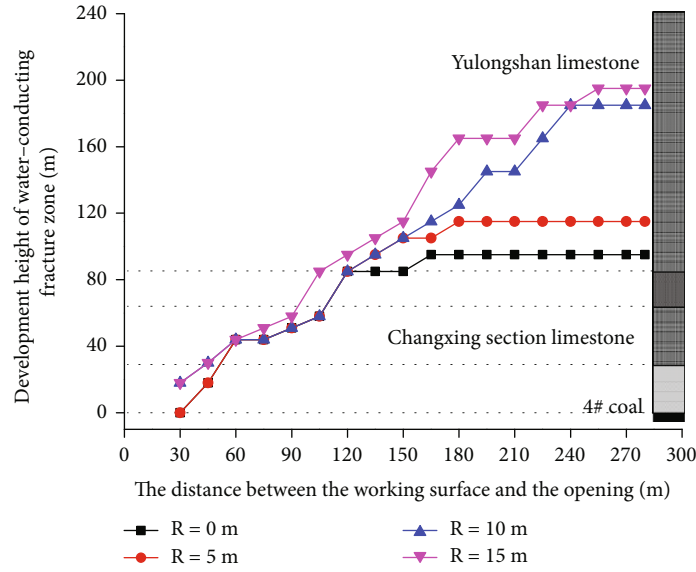


FIGURE 10: Development heights of water-conducting fissures under karst caves with different RADII.

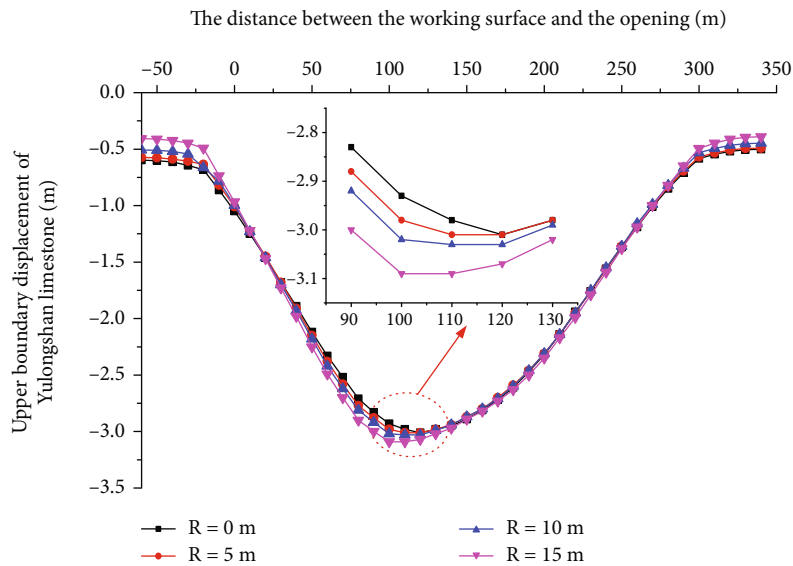


FIGURE 11: Subsidence displacement of limestone top interface in Jade Dragon Snow Mountain.

(2) The radius of the karst cave is 10 m

When the working face is advanced by 45 m, the water-conducting fissured zone develops to a height of 30 m, and the fissures develop to the interior of the Yulongshan limestone; when the working face is advanced by 120 m, the water-conducting fractured zone develops to a height of 95 m, and the fissures develop to the interior of the Yulongshan limestone; when the working face is advanced by 280 m, the water-conducting fissure is connected to the karst cave in the lower part of Yulongshan, and a perturbation through the fissure is formed between the upper and lower karst caves, and the water-conducting channel from the karst cave to the working face is formed. Water-conducting fissures are generated around karst caves affected by mining disturbances, and the karst caves are connected through hor-

izontal and vertical water-conducting fissures to achieve internal hydraulic exchange. The development characteristics of water-conducting fissures when the karst cave is 10 m are shown in Figure 8.

(3) The radius of the karst cave is 15 m

When the working face is advanced by 45 m, the development height of the water-conducting fissured zone is 30 m; when the working face is advanced by 120 m, the development height of the water-conducting fracture zone is 105 m. The evolution characteristics of overburden fissures and mining water-conducting fissures during the excavation of the 4# coal seam with a radius of 15 m and a radius of 10 m are similar for the circular karst cave. However, when the working face advances by 280 m, the disturbance fissures

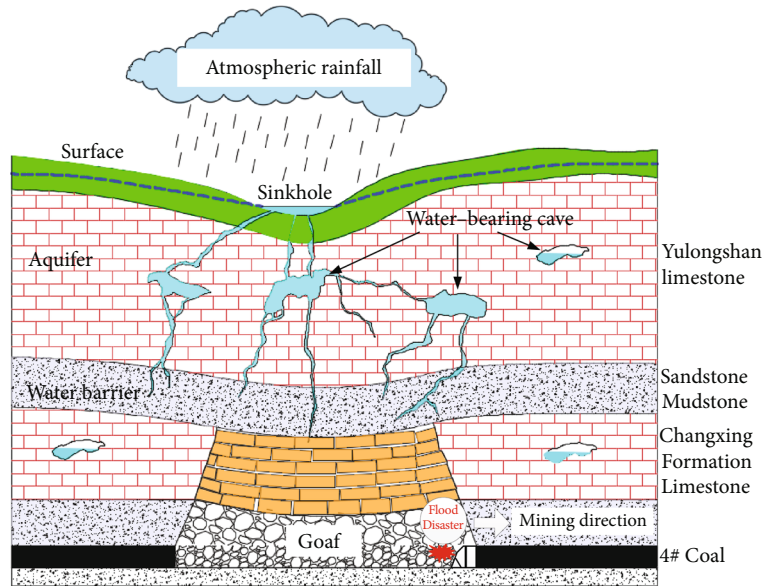


FIGURE 12: Schematic diagram of water inrush process in karst area.

around the karst cave with a radius of 15 m are more developed. The development characteristics of water-conducting fissures when the karst cave is 15 m are shown in Figure 9.

(3) Comparative analysis of the development height of water-conducting fissures

Through the comparative analysis, it is obvious that the maximum height of overlying fissures developed in coal seam mining is positively correlated with the radius of the karst cave. The development height of the water-conducting fractured zone formed by the mining disturbance gradually increases as the radius of the karst cave increases. When the cavern radius is 10 m and 15 m, the height of water-conducting fissures is 185 m and 195 m, and the split mining ratio is 61.7 and 65, respectively. Under the influence of mining, the water-conducting fissures between the water-bearing cavern and the mined-out area are connected, and the water-gushing disaster occurs immediately at the working face. The development heights of water-conducting fissures under karst caves with different RADII are shown in Figure 10.

5.2. Influence of Karst Cave on Overburden Displacement.

Displacement measuring lines are arranged on the roof of the coal seam and the limestone roof of Yulongshan. The subsidence curve of the top interface of the limestone in Yulongshan is shown Figure 11. With the increase of the radius of the karst cave, the maximum subsidence displacement value continues to increase. Therefore, the existence of karst caves affects the development of water-conducting fissures in the Yulongshan limestone aquifer, and the subsidence of the ground corresponding to the working face. Besides, the roof subsidence curve after 280 m of excavation of the 4# coal seam is obtained. With the change in the radius of the karst cave, there is not much difference in the amount of subsidence. The main reason is that the karst cave

is far away from the 4# coal seam, and the stress change generated by the karst cave does not affect the change in the roof displacement of the coal seam.

5.3. Analysis of Water Inrush Disaster. The aquifer under the roof of coal seam in the mining area is made up of Yulongshan limestone and Changxing limestone, and the water supply of the aquifer is mainly atmospheric rainfall. Based on the analysis of mine water consumption and numerical simulation results, it is obvious that the atmospheric rainfall in the karst area mostly enters the underground karst aquifer through water drop holes and karst fissures, which becomes the potential threat of coal mining in the karst area. With the continuous increase of coal mining space, the water-conducting fissure gradually develops upward. The mining disturbance influence on the karst cave in the roof gradually strengthens, and the karst fissure around the cave gradually expands outward. When the mining-induced fissure and karst fissure around the cave conduct, forming a water channel between the cave and the goaf. Due to the influence of mining disturbance, the karst fissure between the karst caves leads to the formation of hydraulic exchange. Therefore, a water channel between the ground surface, the karst cave, and the goaf is formed, shown in Figure 12.

6. Conclusions

- (1) Through the curve analysis of mine water inflow, working face water inflow, and atmospheric rainfall, it is obtained that both mine water inflow and working face water inflow are positively correlated with atmospheric rainfall, which proves that the working face and the ground form a through-type water channel. At the same time, it is verified that the empirical calculation formula for water-conducting fractured zones is not suitable for karst mining areas, and the actual development height of water-

conducting fractured zones in karst areas is larger than the calculation value of the empirical formula

- (2) The numerical simulation results show that with the increase of the radius of the karst cave, the development height of the water-conducting fractured zone of the overlying rock strata increases. The more the karst cave is disturbed by coal mining, the more karst fissures are generated around it. The change in the radius of the karst cave does not affect the subsidence displacement of the coal seam roof and has little effect on the overall structure of Yulongshan. The ground subsidence increases slightly with the increase of the radius of the karst cave
- (3) When the radius of the karst cave is 10 m and 15 m, the split-mining ratio is 61.7 and 65, respectively, and the mining-induced fissure intersects with the karst fissure around the cave. The mining-induced fissure is connected between the cave and the mined-out area of the working face and between the adjacent caves. The water diversion channel is formed between the ground surface, the karst cave, and the mined-out area. Therefore, the atmospheric precipitation flows into the coal mine through the water diversion channel, which verifies the correctness of the positive correlation between the mine water inflow and atmospheric rainfall

Data Availability

The data used to support the findings of this study are included within the article.

Conflicts of Interest

The authors declare that they have no conflicts of interest.

Acknowledgments

This work was supported by the National Natural Science Foundation of China (52174073 and 51774110) and the Natural Science Foundation of Henan Province (222300420007).

References

- [1] J. L. Xu, "Research and progress of coal mine green mining in 20 years," *Coal Science and Technology*, vol. 48, no. 9, pp. 1–15, 2020.
- [2] L. M. Fan, X. D. Ma, Z. Q. Jiang, K. Sun, and R. J. Ji, "Review and thirty years prospect of research on water-preserved coal mining," *Coal Science and Technology*, vol. 47, no. 7, pp. 1–30, 2019.
- [3] Z. Z. Cao, Y. F. Xue, H. Wang, J. R. Chen, and Y. L. Ren, "The non-Darcy characteristics of fault water inrush in karst tunnel based on flow state conversion theory," *Thermal Science*, vol. 25, no. 6, pp. 4415–4421, 2021.
- [4] X. G. Tang, "Occurrence regularities of coal resources in Guizhou Province," *Coal Geology & Exploration*, vol. 40, no. 5, pp. 1–5, 2012.
- [5] Y. Xue, J. Liu, X. Liang, S. Wang, and Z. Ma, "Ecological risk assessment of soil and water loss by thermal enhanced methane recovery: numerical study using two-phase flow simulation," *Journal of Cleaner Production*, vol. 334, article 130183, 2022.
- [6] X. Z. Wang, J. L. Xu, and W. B. Zhu, "Influence of primary key stratum structure stability on evolution of water flowing fracture," *Journal of China Coal Society*, vol. 37, no. 4, pp. 606–612, 2012.
- [7] X. J. Hu, W. P. Li, and D. T. Cao, "Index of multiple factors and expected height of fully mechanized water flowing fractured zone," *Journal of China Coal Society*, vol. 37, no. 4, pp. 613–620, 2012.
- [8] T. F. Liu, "Analysis on the development height and influencing factors of water diversion cracks in coal mining," *Coal Geology & Exploration*, vol. 41, no. 3, pp. 34–37, 2013.
- [9] Y. G. Yang, J. Wang, and Y. J. Yu, "Influence of safe mining sequence of multi coal seams under the river on the height of water diversion fracture zone," *Journal of China Coal Society*, vol. 40, no. s1, pp. 27–32, 2015.
- [10] H. R. Rong, D. L. Wang, J. Y. Gu, and H. Dong, "Effects of valley and slope angles on movement laws of water flowing fracture in roof of shallow buried extra thick coal seam," *Safety in Coal Mines*, vol. 49, no. 11, pp. 63–68, 2018.
- [11] Z. S. Wu, S. Q. Wang, T. Peng, and X. K. Wang, "Numerical simulation on influencing factors of water flowing fractured zone development in Caojiatan coal mine," *Science Technology and Engineering*, vol. 19, no. 25, pp. 125–129, 2019.
- [12] H. Hu, J. G. Ning, J. Wang, G. B. Li, and X. S. Shi, "Numerical simulation on height of water flowing fractured zone development in overlying rocks under hard roof coal seam group mining," *Safety in Coal Mines*, vol. 47, no. 5, pp. 45–48, 2016.
- [13] C. Q. Zhu, D. G. Cui, Z. Zhou, Q. F. Li, and Y. J. Huang, "similarity simulation of mining fissure development and cave failure characteristics in karst mining area," *Chinese Journal of Underground Space and Engineering*, vol. 15, no. 1, pp. 93–100, 2019.
- [14] Y. P. Zhang, Y. J. Zhang, Y. T. Liu, Y. J. Song, and Q. Y. Zhao, "Research on overburden failure height of large-cutting height fully mechanized face in deep thick coal seam in western Mengxi," *China Safety Science Journal*, vol. 30, no. 8, pp. 37–43, 2020.
- [15] W. B. Guo, G. Z. Lou, and B. C. Zhao, "Research on the height of water-conducting fracture zone in top coal caving mining with soft and hard overlying strata in Lugou coal mine," *Journal of Mining & Safety Engineering*, vol. 36, no. 3, pp. 519–526, 2019.
- [16] D. M. Yang, W. B. Guo, G. B. Zhao, Y. Tan, and W. Q. Yang, "Development height of water-conducting fracture zone in fully mechanized caving mining under thick loose layer and weak overburden," *Journal of China Coal Society*, vol. 44, no. 11, pp. 3308–3316, 2021.
- [17] L. Q. Shi, H. B. Wu, Y. L. Li, and W. K. Li, "PCA-GA-Elman optimization model for predicting the development height of water-conducting fracture zone," *Journal of Henan Polytechnic University (Natural Science Edition)*, vol. 40, no. 4, pp. 10–18, 2021.
- [18] T. Li, Y. Gao, D. C. Ai, and J. W. Yang, "Geological model of water preserved mining in karst mountain areas in Southwest China," *Journal of China Coal Society*, vol. 43, no. 3, pp. 747–754, 2018.

- [19] X. Z. Shi, Z. W. Qian, T. W. Li, Z. Q. Jiang, and T. Jiang, "Study on occurrence characteristics of karst ground water in coal stratum roof," *Coal Engineering*, vol. 49, no. 1, pp. 63–66, 2017.
- [20] Y. Xue, J. Liu, P. G. Ranjith, Z. Zhang, F. Gao, and S. Wang, "Experimental investigation on the nonlinear characteristics of energy evolution and failure characteristics of coal under different gas pressures," *Bulletin of Engineering Geology and the Environment*, vol. 81, no. 1, 2022.
- [21] Z. Z. Cao, Y. Wang, H. X. Lin, Q. Sun, X. G. Wu, and X. S. Yang, "Hydraulic fracturing mechanism of rock mass under stress-damage-seepage coupling effect," *Geofluids*, vol. 2022, Article ID 5241708, 11 pages, 2022.